Title
SERRATED YIELDING IN ORDERED AND ORIGINALLY DISORDERED Cu3Au

Authors
Mohamed, F.A.
Murty, K. Linga.
Dorn, J.E.

Publication Date
1971-11-01

Submitted to Philosphical Magazine

SERRATED YIELDING IN ORDERED AND ORIGINALLY DISORDERED Cu_3Au

F. A. Mohamed, K. Linga Murty and J. E. Dorn

November 1971

AEC Contract No. W-7405-eng-48

DISCLAIMER

LBL-193

SERRATED YIELDING IN ORDERED AND ORIGINALLY DISORDERED Cu_3Au

F. A. Mohamed*, K. Linga Murty** and J. E. Dornt
Inorganic Materials Research Division
Lawrence Berkeley Laboratory
University of California, Berkeley

ABSTRACT

The characteristics of serrated flow are studied in both ordered and originally disordered Cu_3Au and three types of serrations (A, B and C) are distinguished in both states of the alloy. The activation energy for types A and B is found to be 17.89 k Cal/mole for the disordered state and that for type A in the ordered alloy is 22.09 k Cal/mole. These values are identified to be the activation energies for vacancy migration in this alloy. $(m + \beta)$ values in the modified Cottrell equation are determined to be 2.18 and 2.98 for disordered and ordered states respectively. These values are in essential agreement with theoretical predictions as well as experimental findings in other alloy systems. Temperature dependence of the disappearance of serrations is studied in both the states and thus obtained activation energy values (42.72 and 52.84 k Cal/mole for disordered and ordered respectively) are identified to be the sum of the self-diffusion energy and the binding energy of solute atom with dislocations in Cu_3Au.

*Research Assistant

**Research Associate

†Senior Scientist and Professor of Materials Science of the College of Engineering, University of California, Berkeley, California; deceased September 1971.

A study of the temperature dependence of yield stress revealed no simple correlation with the characteristics of serrated flow. The yield stress and its temperature dependence are believed to have resulted from the simultaneous preponderance of an athermal stress due to solid-solution hardening and that due to ordering; change in the degree of order for the ordered case while short-range ordering in originally disordered alloy. Although a peak in strain-hardening coefficient versus temperature plot was observed for the ordered alloy, no correlation with serrated flow was noted. In addition only temperature-insensitive $\frac{d\sigma}{d\epsilon}$ was observed in the disordered case. Thus no meaningful correlation of these findings with the strain-ageing behavior could be made in this alloy. However these observations on the temperature dependence of strain-hardening coefficient are in line with earlier experiments.

1. INTRODUCTION

Within certain ranges of temperatures and strain-rates serrated stress-strain curves have been observed for metals and, both substitutional and interstitial solid solution alloys. This phenomenon of serrated yielding and flow, generally referred to as the Portevin-Le Chatelier effect has been observed in several alloys and at present a vast amount of literature is available on this subject. These serrations are believed to arise from solute atom dislocation interactions which may be classified into two major groups: (i) athermal effects of clusters of solute atoms (Fisher (1954)), and short and long range ordering (Cottrell (1953), G. H. Ardley (1955)); and (ii) thermally activated process associated with Suzuki (1952) and Cottrell (1948) locking of dislocations. Majority

of experimental evidence suggests that Cottrell locking of moving dislocations to solute atoms is responsible for the appearance of jerky flow. If the temperature is high enough so that solute atmospheres can migrate with dislocations, the atmospheres can 'catch up' with slowly moving dislocations and cause them to decelerate, finally locking them completely. In contrast 'fast' dislocations will leave their atmospheres and continue to accelerate. In this way it might be possible to account for the serrated steps observed in stress-strain curves of solid solution alloys. Cottrell theory, with slight modifications was applied by several investigators to quantitatively explain the observation of serrations and other details as well as the resulting activation energies for jerky flow in various alloy systems (Russell (1963), Nakada and Keh (1970), Ham and Jaffrey (1967), Brindley and Worthington (1969), Mukherjee, D'Antonio, Maciag and Fisher (1968), Charnock (1969), MacEwen and Ramaswami (1970), McCormick (1970)).

In a recent investigation Langdon and Dorn (1968) demonstrated that the deformation of Cu_3Au seemed to be controlled by Peierls mechanism over the low temperature region extending up to about 100°K for ordered and 330°K for disordered. Above about 370°K originally disordered Cu_3Au exhibited serrated stress-strain curves somewhat similar to those attributable to dynamic strain-ageing (Cottrell (1953)b). On this basis it appears likely that these serrations should be observed in ordered alloy as well, since the pertinent factors of solute-atom diffusion and interaction with dislocations should also be operative in ordered Cu_3Au. Present investigation was undertaken to make a detailed study of the

serrated yielding in both disordered and ordered Cu_3Au, the types of serrations and their dependencies on various parameters such as the imposed strain-rate, temperature etc. Although Langdon and Dorn (1968) did not observe serrated yielding in ordered alloy at the temperatures and strain-rates employed there, it will be demonstrated in the present study that at suitable strain-rates and temperatures serrated flow was observed in both ordered and originally disordered alloys. In addition it is found here that the characteristics of serrations in ordered and disordered Cu_3Au are similar and can be accounted for by dynamic strain-ageing.

2. THEORY

Theories put forward to explain the appearance and other details of serrations in stress-strain curves may be broadly classified into two categories based on (i) dislocation multiplication concept (Johnston and Gilman (1959)) and (ii) Cottrell's dynamic strain-ageing hypothesis.

(1) Johnston-Gilman Approach:

Initial yield points in certain materials could be explained in terms of the rapid multiplication of dislocations. This idea may be extended to serrated yielding by visualizing each stress-drop to be due to some sudden dislocation multiplication. In a tensile test the extension rate imposed by the machine is balanced by the sum of the elastic and plastic strain rates of the specimen so that

$$\dot{\varepsilon}_x = \frac{1}{E}\frac{d\sigma}{dt} + \frac{1}{2}\rho_m \, b\bar{v} \qquad (1)$$

where $\dot{\varepsilon}_x$ is the cross-head speed, E the effective modulus, ρ_m the mobile dislocation density, b the Burger's vector and $\bar{v}$ the mean dislocation

velocity. A rapid rise in ρ_m due to the operation of a source results in a drop in the average velocity. Since the dislocation velocity is related to the stress through (Johnston and Gilman (1959))

$$\bar{v} = \left(\frac{\tau}{\tau_o}\right)^n \quad , \tag{2}$$

a resultant drop in stress is realized. As dynamic strain-ageing occurs and $\bar{v}$ decreases due to solute-locking, the stress passes through a minimum and again increases at a rate determined by the rate of ageing and by the stiffness of the machine. Again when stress increases to a level where another source can operate, ρ_m increases. Thus repeated source operation and dynamic strain-ageing will result in serrated stress-strain curves. Qualitatively therefore the appearance of serrations can be accounted for. But it is not clear how one can deduce the effect of temperature and strain-rate on the observed delay of strain for the onset of serrations and activation energies for flow, etc., based on this model.

(2) Cottrell's Model:

In Cottrell's model the solute responsible is considered to diffuse fast enough to keep up with freely moving dislocation by forming an atmosphere around them. The stress then rises until the dislocations break away from their solute atmospheres. Repetition of such a process results in jerky or serrated flow. The average velocity of solute atom at distance r is given by

$$V = \frac{D}{kT}\ \frac{A}{r^2} = \frac{D\ell}{r^2} \tag{3}$$

where V = velocity of solute atom

A = interaction constant

D = diffusion coefficient of the solute

and $\ell = \frac{A}{kT}$ = 'effective radius' or the characteristic length of the atmosphere. Assuming a dilute concentration of solute, Cottrell (1953b) approximates

$$\ell = 2r \tag{4}$$

so that the 'critical' velocity for the dislocation to escape its atmosphere is given by

$$V_c = \frac{4D}{\ell} \quad . \tag{5}$$

This critical velocity fixes the critical imposed strain-rate to be

$$\dot{\varepsilon}_c = \rho_m \, bV_c = \frac{4D \, \rho_m b}{\ell} \quad , \tag{6}$$

where ρ_m and b are movile dislocation density and Burger's vector respectively. Thus if the imposed strain-rate

$$\dot{\varepsilon} = \rho_m \, bv < \frac{4D \, \rho_m b}{\ell} = \dot{\varepsilon}_c \quad , \tag{7}$$

the atmosphere drags behind the dislocation; and if

$$\dot{\varepsilon} > \dot{\varepsilon}_c \tag{8}$$

the dislocation can escape and leave its atmosphere. Thus once dislocations get 'stuck' with their atmospheres the stress rises sufficiently to acquire $\dot{\varepsilon} = \rho bv > \dot{\varepsilon}_c$ and then the dislocations get 'freed.' These freely moving dislocations can be repeatedly locked by solute atoms and unlocked by stressing thereby rendering the stress-strain curve serrated.

In the temperature region where jerky flow was observed the diffusivity of solute atoms is too low to give this effect in substitutional alloys. But Cottrell (1953b) pointed out that since a finite plastic strain was

always observed before the serrations occur, the diffusion coefficient will be enhanced by a non-equilibrium excess vacancy concentration due to straining. In addition he observed this initial strain to be temperature and strain-rate dependent and thus incorporated, in his theory, this delay in strain (ε_o) as a requisite to create sufficient concentration of vacancies in excess of equilibrium number to enhance the diffusivity of solute atoms enabling thereby their interaction with moving dislocations. Following Seitz (1952) and Mott (1952), diffusivity assisted by vacancies is given by

$$D = b^2 Z \nu_o C_v e^{-g_m/RT} \quad , \tag{9}$$

where

Z = Coordination number

ν_o = Debye frequency

C_v = Vacancy concentration

g_m = Gibbs free energy of activation for vacancy migration

and RT = product of Gas constant and absolute temperature.

In general

$$C_v = C_v^T + C_v^\varepsilon \quad , \tag{10}$$

where C_v^T is the thermal equilibrium vacancy concentration at temperature T and C_v^ε the excess vacancy concentration due to straining at strain ε. With Eq. 9 for diffusivity the critical strain-rate $\dot{\varepsilon}_c$ becomes

$$\dot{\varepsilon}_c = \frac{4\,b}{\ell}\ \rho_m D = K \rho_m C_v e^{-E_m/RT} \quad , \tag{11}$$

where $K = \dfrac{4\,b^3 \nu_o Z}{\ell}$, assuming a negligible entropy-contribution. Or

$$\ln \dot{\varepsilon}_c = \ln K + \ln \rho_m + \ln C_v - \frac{E_m}{RT} \quad . \tag{12}$$

Eq. 12 brings out the need for further elucidation of two important parameters in Cottrell's approach, namely the mobile dislocation density (ρ_m) and the 'total' vacancy concentration (C_v). Various investigators related these two factors to the delay of plastic strain (ε_o) observed before the first jerk starts.

(2a) Vacancy Concentration-Strain Relation:

In general the excess vacancy concentration due to straining may be represented as (Seitz (1952), van Bueren (1955))

$$C_v^{\varepsilon} = B\ \varepsilon^m \quad . \tag{13}$$

From resistivity measurements on Al alloys Seitz (1952) obtained $B = 10^{-4}$ and $m = 1$ in the above equation. Van Bueren (1955) considered the intersection of two screw dislocations leading to the formation of a jog on each dislocation capable of producing point defects as these dislocations move ahead. By considering single as well as multiple glide he predicted the range of m values to be

$$1.25 \leq m \leq 2 \quad ,$$

the lower limit being obtained for single glide and the upper for multiple. His analysis yields a value of about '$3.25 \times 10^{10}\ \Omega$' for B in Eq. 13, where Ω is the atomic volume. A similar relationship with $B = 9 \times 10^{-2}$ and $m = 1$ can also be obtained following an analysis of creation of vacancies at vacancy producing jogs on gliding screws (Wazzan and Dorn (1965)). Blewitt et al (1955) observed a parabolic increase in resistivity with strain in Cu crystals at liquid helium temperature while Bolling (1959) obtained a value of 1.36 for 'm' from experiments on α-Brass. All these prove the nominal validity of Eq. 13. However, in these analyses

it was assumed that there is no recovery: once formed a vacancy never anneals out to a sink. This is definitely invalid especially at higher temperatures where vacancy diffusion is fast enough. This annealing of vacancies to appropriate sinks has been recently considered by Murty and Dorn (1971) who demonstrated that this is of significance in some cases and quantitatively explained the deviations from Cottrell model observed by MacEwen and Ramaswani (1970).

(2b) Mobil Dislocation Density-Strain Relation:

The mobile dislocation density may be related to plastic strain. Johnston and Gilman (1959) obtained the following relation from their mechanical measurements:

$$\rho_m = 10^9 \, \varepsilon^{\beta} \quad , \beta = 1 \quad . \tag{14}$$

Ham and Jaffrey (1967) on the other hand were able to establish, from their experiments using transmission electron microscopy in tin-bronze alloys, the proportionality

$$\rho \propto \varepsilon^{1.17} \quad . \tag{15}$$

This is the total dislocation density and in general ρ_m can be taken as a constant fraction of the total density so that

$$\rho_m \propto \varepsilon^{\beta} \quad \beta \gtrsim 1 \quad . \tag{16}$$

It is believed on the other hand that the dislocation density (ρ) depends on flow stress rather than strain (Bird, Mukherjee and Dorn (1969)). Rider and Faxon (1966) found for Al, the relation between the total dislocation density and the flow stress to be

$$\sigma = K_1 \sqrt{\rho} \tag{17}$$

while that between the stress and strain to be

$$\sigma = K_2 \sqrt{\varepsilon} \quad , \tag{18}$$

or the value of β in Eq. 14 is unity in agreement with Johnston-Gilman data.

From the above two subsections we find that Coltrell's equation can be rewritten as

$$\ln \dot{\varepsilon}_c = \ln K + (m + \beta) \ln \varepsilon_o - \frac{E_m}{RT} \quad , \tag{20}$$

from which one finds that (i) at constant temperature $\ln \dot{\varepsilon}_c$ and $\ln \varepsilon_o$ are linearly related with a slope equal to $(m + \beta)$ and (ii) if one plots $\ln \dot{\varepsilon}_c$ vs T^{-1} at constant ε_o or $\ln \varepsilon_o$ vs T^{-1} at constant $\dot{\varepsilon}_c$, one should obtain the activation energy for motion of vacancies. Of course Eq. 20 and the above predictions are valid only at temperatures low enough so that

$$C_v^T << C_v^\varepsilon \quad . \tag{21}$$

Otherwise thermal equilibrium vacancy concentration should also be considered. In such a case we find a more complicated expression for $\dot{\varepsilon}_c$ in place of Eq. 20, namely

$$\ln \dot{\varepsilon}_c = \ln K' + \beta \ln \varepsilon_o + \ln \left(e^{-E_f/RT} + B\, \varepsilon_o^{\,m}\right) - \frac{E_m}{RT} \, , \tag{22}$$

so that

$$\left(\frac{\partial \ln \dot{\varepsilon}_c}{\partial \ln \varepsilon_o}\right)_T = \beta + \left(\frac{m \beta \varepsilon_o^{\,m}}{e^{-E_f/RT} + B\, \varepsilon_o^{\,m}}\right)_T \quad ,$$

$$-\left[\frac{\partial \ln \dot{\varepsilon}_c}{\partial (1/RT)}\right]_{\varepsilon_o} = E_m + \left(\frac{E_f\, e^{-E_f/RT}}{e^{-E_f/RT} + B\, \varepsilon_o^{\,m}}\right)_{\varepsilon_o} \quad , \tag{23}$$

and

$$\left[\frac{\partial \ln \varepsilon_o}{\partial (1/RT)}\right]_{\dot{\varepsilon}_c} = \frac{E_m B \varepsilon_o^m + (E_f + E_m)\, e^{-E_f/RT}}{B (m + \beta) \varepsilon_o^m + \beta\, e^{-E_f/RT}}$$

Various parameters in Eq. 22 above can be obtained from an analysis of the experimental data of ε_o, $\dot{\varepsilon}_c$ and T. Equations 23 lead to simpler ones used by various investigators obtained from Eq. 20 at low temperatures. MacEwen and Ramaswami (1970) consider expressions similar to 23a and 23c above and attempt to qualitatively explain some of the deviations in their plot "ln ε_o vs 1/T" at higher temperatures of their results on single crystals of Al-Mg alloy. Inclusion of annihilation of vacancies at sinks leads to still complicated expression for $\dot{\varepsilon}_c$ in lieu of Eq. 22 namely (Murty and Dorn (1971)).

$$\ln \dot{\varepsilon}_c = \ln K' + \beta \ln \varepsilon_o + \ln \left\{ e^{-E_f/RT} + B' \left(\varepsilon_o - \frac{4 D_v \rho}{3 \dot{\varepsilon}_c} \varepsilon_o^2 \right) \right\} - \frac{E_m}{RT} , \tag{24}$$

where B' is a constant and ρ is the dislocation density.

3. EXPERIMENTAL TECHNIQUES

In the course of this investigation the heat of Cu_3Au was cast into a graphite mold, forged to 0.75 in. in diameter and finally cold swaged to $\frac{1}{8}$ in. rods. Tensile test specimens of 0.085 in. in diameter having 0.68 in. long gage section were then machined from these rods.

The disordered state was achieved by annealing under argon at 1000°K for 30 min. for the dual purpose of further homogenizing the specimens and providing a stable grain size. Specimens were next slowly cooled to 725°K (62°K above T_c) over 2 hours, then held there for about 15 min, and finally quenched in water at room temperature. The efficiency of quench is evident by the fact that in no case even the faintest trace of super lattice lines could be detected in the Debye-Scherrer photograms. Specimens for the ordered state were also annealed under argon at 1000°K for about 30 min., furnace cooled below the ordering temperature (663°K)

to 643°K, held at this temperature for 85 hours, and then slowly cooled to room temperature. Metallographic examination following etching with a 50% aqueous solution of I_2 in KI revealed that both the disordered and ordered states had the same grain size with about 630 grains per cm.

All tensile tests were conducted on an Instron testing machine. For tests above the room temperature the tensile test specimens were completely immersed in continuously agitated and thermostatically controlled silicone oil baths. Temperature remained within $\pm$ 1° of the reported values. Tensile tests were performed at temperatures between 163°K and 650°K with the nominal strain-rate in the range of 10^{-5} to 10^{-3} sec^{-1}.

Stresses were calculated from tensile loads and cross sectional areas, to an accuracy of $\pm$ 0.1 x 10^8 dynes/cm^2. Strains deduced from the elongation data and initial gage lengths are accurate to better than 0.002. When required the true strains and true stresses were calculated from the following equations

$$\epsilon = \ln \frac{L}{L_o} = \ln (1 + e)$$

$$\sigma = \sigma_o (1 + e)$$

where

ϵ = true strain

e = normal extension

σ = true stress

σ_o = nominal stress

4. EXPERIMENTAL RESULTS

(1) Characteristics of Serrations:

Typical load-extension curves for a series of tension tests at a

machine cross-head speed of 0.02 in/min or $\dot{\varepsilon} \approx 4.57 \times 10^{-4}$ sec^{-1} from 320 to 648°K for disordered and from 380 to 633°K for ordered Cu_3Au are presented in Figs. 1 and 2 respectively. Serrations, appeared in these curves, may be classified into 3 types, named types A, B and C. It is interesting to note that thus far in any material, investigators reported at most two of these 3 types and in no case other than the present one all these 3 types have been reported or could be distinguished.

Types A and B were similar to those first reported by Russell[8] in a study on copper-tin alloys. Type A known as 'periodic' due to its regularity is characterized by the size of the yield drop ($\Delta\sigma$) increasing with an increasing amount of plastic strain and thus the ageing time between successive yield points. Type B called 'fine' appears at relatively higher strains and is superimposed on type A serrations. Type C is characterized by having a yield drop always below the general level of the stress-strain curve in contrast to A and B which show yield drops above, and oscillating above and below the curve respectively. Type C serrations, observed at relatively high temperatures and when the serrations were about to disappear, are identical to those very recently reported by Soler-Gomez and Tegart (1969) in Au-In alloys. All these three types of jerky flow are illustrated in figures 1 and 2. All of these were observed in <u>both</u> ordered and disordered Cu_3Au. As shown in Fig. 2, type B did not appear in ordered alloy at the illustrated temperatures but was observed at a temperature of 457°K and a strain-rate 4.57×10^{-5} sec^{-1}.

The effects of strain on the yield drop ($\Delta\sigma$) and the separation of serrations ($\Delta\varepsilon$) are recorded in figures 3 and 4 while Fig. 5 reveals the dependence of $\Delta\sigma$ on the ageing time. The strain-rate ($\dot{\varepsilon}$) dependencies

of the strain (ε_o) to the onset of serrations are shown in Fig. 6 for both ordered as well as disordered states. These double-log plots reveal the validity of Eq. 20 for both cases although the slopes are different for ordered and disordered alloys: 2.18 and 2.98 for disordered and ordered Cu_3Au respectively. As will be seen later, these values are comparable to those reported for other materials.

Results of an investigation of the effect of temperature on ε_o for the onset of serrations are shown in Fig. 7. For disordered Cu_3Au datum points are plotted for both type A as well as B while in the case of ordered state only for type A since in this ordered alloy type B serrations either do not appear or cannot be distinguished from background, in the temperature range employed here. Again a nice correlation with Eq. 20 is noted. Slopes of the Arrhenius plots in Fig. 7 yield an average value of 4.13 ± 0.18 for the disordered alloy and 3.73 ± 01 for the ordered. These slopes combined with $(m \pm \beta)$ values obtained from $\ln \dot{\varepsilon}$ vs $\ln \varepsilon_o$ plots gave the following results for the activation energy for serrated flow:

$$E_m = 17.89 \pm 0.78 \text{ k Cal/mole for disordered}$$

and

$$E_m = 22.09 \pm 0.06 \text{ k Cal/mole for ordered.}$$

(2) Disappearance of Serrations:

The temperatures and the corresponding strain-rates at which the serrations <u>just</u> disappear from the stress-strain curves and at which completely smooth curves are found were investigated for both the states. Fig. 8 is a plot of logarithm of strain-rate versus the reciprocal of absolute temperature for disappearance of jerky flow. This disappearance is also found to be thermally activated similar to the findings of Keh

et al (1968) in interstitial solute atom-locking. The resulting slopes of these Arrhenius plots yielded values for the activation energy for disappearance (Q') of serrations to be

$$Q' = 42.72 \pm 1.65k \text{ Cal/mole for disordered}$$

and (26)

$$Q' = 52.84 \pm 1.56k \text{ Cal/mole for ordered.}$$

(3) Temperature and Strain-Rate Dependence of Deformation Characteristics: These results are presented in two parts: one pertaining to originally disordered Cu_3Au and the second one to ordered state.

(i) Disordered Cu_3Au: From the documented variation of yield stress with temperature in Fig. 9 we note an athermal behavior in the range 375 to 450°K where the yield stress is insensitive to both the temperature and strain-rate. At around 450°K it starts to increase rapidly until about 475°K from when on the stress increased slowly. Over the region of increasing yield stress (450 -585°K) lower strain-rate yielded higher stress values revealing the existence of a slight 'negative-temperature' effect. And, at still higher temperatures above about 585°K higher strain-rate data gave higher stresses. Shown in Fig. 10 is the temperature independence of strain-hardening coefficient, $(\frac{d\sigma}{d\epsilon})$. Above about 0.001 strain, the stress-strain curves are all linear and thus the slopes of these lines are taken as the measure of the strain-hardening coefficient. Thus the variation of flow stress at strains beyond 0.001 is identical to the temperature dependence of the yield-stress, taken at 0.002 off-set from the modulus lines. The range of temperatures and whether the curves are serrated or not in these ranges are tabulated below for clarity (Table 1). Although a slight negative-temperature region is observed between 450 -

585°K, there seems to be no correlation of this finding with the appearance of serrations. Moreover, it is interesting to note that there exists no additional strain-hardening in the serrated region in contrast to findings in some interstitial solid solution alloys (Keh, Nakada and Leslie (1968)).

(ii) Ordered Cu_3Au: As revealed in Fig. 9, below 380°K an athermal behavior was observed. Above about 380°K, yield stress increases first gradually and then the rate of increase in stress with temperature increases as temperature increases. There is no evidence of negative temperature region. On the other hand, the strain-hardening coefficient as a function of temperature revealed a peak (Fig. 10) at about 300°K at which temperature no serrated stress-strain curves were observed at the strain-rates employed here. It is to be noted that as Curie temperature is approached, both ordered and disordered alloys seem to give identical values for the yield stress as well as for $\frac{d\sigma}{d\varepsilon}$, as expected. Again various regions of temperatures are tabulated in Table 1 for the ordered case also.

It might be of significance to note that in the case of disordered alloys, no superlattice lines could be detected up to about 596°K while faint lines were found in the specimens tested at 614 and 648°K.

5. DISUCSSION

Originally-disordered as well as ordered Cu_3Au alloys were tested below the curie temperature of order-disorder transformation. As seen in the previous section, in some ranges of temperatures the stress-strain curves of both types of alloys are serrated in contrast to the earlier observation by Langdon and Dorn (1968). These serrations were grouped into 3 types (A, B and C), and in the present section, we will attempt to

put all the experimental observations together to compare with various theoretical models.

In general, in a material such as disordered Cu_3Au jerky flow may be attributed to either of the mechanisms: (1) dynamic reordering of short-range-order (SRO) and (2) dynamic strain ageing or solute atom-dislocation interaction. The first possibility is Cottrell's (1953a) development of Fisher's (1954) idea of short range order hardening. When a dislocation passes through a completely disordered alloy the internal energy of the crystal remains unchanged and only a small stress is required to move it. However if there is some short range ordering present (due to either quenching from above the critical temperature or annealing the originally disordered structure below T_c), the stress need be higher to disorder the short range order across the slip plane. After this destruction of SRO the stress necessary to move the second dislocation is smaller, i.e. stress to start deformation is less than that to continue. If the conditions are such that the SRO is allowed to reestablish itself, stress has to be increased to destroy SRO. Repetition of such a process can produce sudden jerks in a stress-strain curve. However, this mechanism is disqualified for the present case of Cu_3Au due mainly to two reasons: (1) serrations observed here have identical characteristics with those observed in substitutional alloys where dynamic strain ageing was operating, and (2) the characterisitics of serrations in both ordered and disordered alloys are similar.

In the following, dynamic strain ageing is considered to explain various experimental findings reported in the last section:

As mentioned earlier the types of serrations observed in both ordered and disordered Cu_3Au are similar to those found in various substitutional alloy systems. Types A and B can be thought to be due to a narrow 'deformation' band passing down the specimen once between each A-type yielding (Russell (1963)). Stress concentration built up in the band will unlock dislocations from their solute atmospheres some of which move rapidly while others, left behind, move relatively slowly. These lagging dislocations will be slowed down further due to the increase in atmosphere as well as the degree of locking and thus the flow stress should rise. Since the stress continues to build up during the propagation of the band some deformation must be taking place behind the band front (Worthington and Brindley (1969)). When the band reaches the end of the gauge length, the number of free dislocations in the specimen is too low to keep the imposed strain-rate. Such a situation leads to generation of new dislocations and produces a new deformation band. A repetition of such a process leads to type A serrations. When type B yielding occurs, the fast moving dislocations in the deformation band age during straining and thus they require higher diffusivity to be unlocked. Thus B-type serrations appear in the stress-strain curves at higher temperatures and/or at higher strains in accordance with experimental findings. To start with, however, these fast moving dislocations are partially aged and thus a superposition of type B on A may result. But as the diffusivity increases due for example to straining, the dislocations get fully aged, the deformation band will be formed randomly and thus the periodicity of type A disappears rendering thereby both types indistinguishable; a fact in harmony with experimental observations.

As noted earlier, yet another form of jerky flow, type C, is observed in the present case. At high enough temperatures where the diffusion rate is such that the solute atoms can migrate with the dislocations, and the balance between the dislocations being 'locked' or 'unlocked' is so critical that any slight deviation from ideality results in catastrophic unlocking (Soler-Gomez and Mc G. Tegart (1969)). This critical nature is manifest by the rapid recovery to the relocked condition and by the way the jerks occur randomly on the stress-strain curve (Figs. 1 and 2). Thus this kind of serrations appears only in a narrow temperature range (Table 1) and this type C can be considered to be due to 'unlocking' (note that these C type are always below the general level of the stress-strain curve) while the type A, due to 'locking' (type A is always above the general level).

(1) Strain-Ageing Kinetics of Type A:

As suggested by Russell (1963) the strain-ageing kinetics of type A serrations can be studied using Cottrell-Bilby (1949) equation. The fraction of total dissolved solute $\frac{n_t}{n_o}$ migrating to dislocations in time t, at a temperature T is given by

$$\frac{n_t}{n_o} = 3\left(\frac{\pi}{2}\right)^{1/3} \rho\left(\frac{ADt}{RT}\right)^{2/3} \quad , \tag{27}$$

where A is the same interaction constant used in Eq. 3. The size of the yield drop ($\Delta\sigma$) can be regarded as proportional to the number of solute atoms migrated to the dislocation and so at a certain strain,

$$\Delta\sigma_t \propto n_t \propto \left(\frac{D}{T}\right)^{2/3} \qquad \text{constant } \varepsilon \text{ or } t \quad ,$$

or

$$\Delta\sigma_t = K' \left[\frac{e^{-E_m/RT}}{T}\right]^{2/3}, \qquad (28)$$

so that a plot of $\ln(\Delta\sigma_t)$ vs $\ln\left(\frac{e^{-E_m/RT}}{T}\right)$ should result in a straight line with a slop equal to 2/3. Indeed such a correlation is seen in Fig. 11 where two different lines were obtained for two different strains and the average slope of these lines is 0.73.

(2) $(m + \beta)$ and Activation Energies:

Figures 6 and 7 reveal the general validity of Cottrell equation, for Cu_3Au, assuming that (i) thermal equilibrium vacancy concentration is negligible compared to that due to straining and (ii) the annealing of vacancies to sinks can be neglected at the temperatures employed here. These assumptions can be shown to be valid here at the temperatures and strain-rates employed. Thermal equilibrium vacancy concentration is

$$C_v^T = e^{-E_f/RT} = 2.05 \times 10^{-10} \quad \text{for disordered } Cu_3Au$$

at the highest temperature where serrations were observed, namely 520°K. Here a value of 23.05 k Cal/mole was used for E_f as found by Benci et al (1964) and also in agreement with the present results, as will be seen later. On the otherhand, the concentration of vacancies due to straining is given by Eq. 13 with $B = 9.43 \times 10^{-2}$ and $m = 1$ so that

$$C_v^\varepsilon = 9.43 \times 10^{-5} \quad \text{for the least value}$$

of ε namely 10^{-3}. If one follows Van Bueren (1955) this value b ecomes 1.72×10^{-5}. In any case in this material even at the highest temperature and least ε_o

$$C_v^\varepsilon >> C_v^T \quad .$$

Experimental data as shown in Figs. 6 and 7 did not reveal any deviations from Eq. 20 supporting the assumed fact that the vacancy annealing in this material has negligible effect on the overall effective vacancy concentration at the strain-rates and temperatures employed here.

Plots of ln $\dot{\varepsilon}$ vs ln ε_o at constant T resulted in straight lines consistent with the modified Cottrell equation. Values of $(m + \beta)$ obtained from these plots are recorded in Table 2 along with those determined for other alloy systems by various authors. As seen here the present values fall in the range of reported ones.

A plot of either ln ε_o or ln $\dot{\varepsilon}$ as a function of 1/T should result in a straight line with slope equal to $\frac{E_m}{(m+\beta)R}$ or $-\frac{E_m}{R}$ respectively. Using the slopes of the Arrhenius plots in Fig. 7 the activation energies for serrated flow in order and disordered Cu_3Au are found to be 22.09 and 17.89 k Cal/mole respectively. Although not shown earlier since only 2 strain-rates were employed the above results are found to be consistent with the plots of ln $\dot{\varepsilon}$ vs T^{-1} the slopes of which yield the activation energy of 17.6 $\pm$ 1.03 for the disordered case (Fig. 12). All these findings support Cottrell theory and are in line with the modified Cottrell equation. The present value of 17.89 k Cal/mole is close to 16.95 found for the migration energy of a vacancy in disordered Cu_3Au by Benci et al (1964) from their experiments on annealing of quenched in resistivity. Thus the present conclusion that the activation energy for serrated flow is identical to that for vacancy motion is in accordance with various studies in different alloys. The energy value for the ordered alloy cannot be compared due to the unavailability of experimental data on

activation energies in the ordered state. However, as will be explained later one expects a slightly higher value for E_m in the ordered alloy compared to that in the disordered.

As demonstrated earlier the disappearance of serrations from the stress-strain curves can also be represented by Arrhenius type of plot (Fig. 8). Keh et al (1968) have shown that the activation energy for disappearance of serrations is given by the sum of the energies for solute diffusion and the binding energy of the solute-atom to dislocations. In the present case of Cu_3Au we obtained values of 42.72 and 52.84 k Cal/mole for the apparent activation energies for disappearance of serrations in disordered and ordered alloys respectively. Benci et al (1964) obtained a value of 1.72 ev (= 39.65 k Cal/mole) for diffusion ($E_m + E_f$) in disordered Cu_3Au so that the difference of 3.07 k Cal/mole may be ascribed to the binding energy of the solute atom with the dislocation in this material. Again no such comparison is possible for the ordered case. However, the same value of 3.07 k Cal/mole may be regarded as the binding energy in the ordered alloy also so that

$$E_D = E_m + E_f = 39.65 \text{ k Cal/mole for disordered}$$

and

$$E_m + E_f \simeq 49.77 \text{ k Cal/mole for ordered.}$$

Thus we find that the ratio of the above values is

$$\frac{E_D^{ord}}{E_D^{dis}} = 1.26 \quad ,$$

which is of the same order as has been found in other alloy systems, and also in the present case for E_m, see Table 3.

Such a trend of higher activation energies in ordered alloys is expected on the grounds that in an alloy with long-range order the disturbance of nearest neighbor relationship requires extra energy.

(3) Temperature and Strain-Rate Dependence of Yield Stress:

Cottrell-Jaswon (1949) model based on dislocation-dragging of solute atmospheres as well as Schoeck-Seeger (1959) theory of yield stress due to Snoek ordering of interstitial solute atoms around dislocations predict a peak in the yield stress versus temperature curve. No experimental support of such a prediction in substitutional alloys in the dynamic strain ageing region is available so far. However such peaks were observed in alloys with intersititial solute atoms such as C or N in Fe. (Keh, Nakada and Leslie (1968)). In iron and steel, at least, dynamic strain ageing is manifested by negative temperature and high work-hardening rates.

In the present case of Cu_3Au the effect of temperature on the yield stress is shown in Fig. 9. In the ordered alloy an athermal behavior of yield stress is found in the region between $\sim$170 and $\sim$350°K and from then on the stress monotonically increased. No serrations were observed in the athermal region and neither a region of negative temperature when serrated yielding occured. Following Ardley (1955) who obtained a similar temperature dependence of yield stress, the increase in the stress beyond 350°K may be attributed to the change in the degree of order, c.f. Fig. 13.

As documented in Fig. 9 yield stress in disordered alloy has a complicated temperature dependence. Such a dependence might be ascribed to short-range ordering reaction. (Mohamed (1970)). Although a region of negative temperature was observed it seems to have no correlation with

the observation of serrations or dynamic strain-ageing since in the temperature range (360°-530°K) where completely serrated stress-strain curves were obtained, part of this region (360-440) has an athermal behavior while the other part has a negative temperature effect of the yield stress. This complicated effect could be due to the simultaneous predominence of both short-range ordering as well as dynamic strain ageing.

It might be interesting to note that Li (1968) after modifying Mott-Nabarro theory of solid-solution hardening, showed that the hardening due to solute atoms is nearly athermal and

$$\tau = 2\mu ef, \quad \text{for small } f,$$

where τ is the shear stress due to solid-solution hardening, μ the shear modulus and e = solute misfit = $\frac{1}{a}\left(\frac{da}{df}\right)$ with a and f being lattice parameter and solute concentration respectively. The yield stress and its temperature dependence observed in both ordered and disordered alloys might have arisen because of the addition of this athermal stress due to solid-solution hardening and that due to ordering - change of degree of order in ordered alloy (Ardley (1955)) and short-range ordering reaction in originally disorderd Cu_3Au (Mohamed (1970)). Mohamed (1970) has shown that a rapid increase in the yield stress between 450 and 480°K is due to the abrupt increase in the absolute degree of short-range order. The slower increase in short-range order between 490 and 550°K was attributed to the fact that the equilibrium value for each temperature here is being approached. Above predictions are still valid since the temperature dependence of the yield stress is unaltered by adding an athermal stress. Same might be true for the ordered case also.

Serrations in the stress-strain curve are believed to enhance dislocation multiplication thereby increasing the strain-hardening. Thus in the region of strain-ageing one expects a maximum in the strain-hardening rate while at lower and higher temperatures strain-hardening coefficient should decrease. Although such a trend seemed to be present in the ordered alloy, only temperature insensitive $\frac{d\sigma}{d\varepsilon}$ was observed in disordered Cu_3Au (Fig. 10). The observations recorded in Fig. 10 are completely identical to the earlier data in single crystals by Stoloff and Davies (1965). At about 630°K the value of $\frac{d\sigma}{d\varepsilon}$ for ordered alloy coincides with that for the originally disordered. These observations may be explained through the mechanism proposed by Stoloff and Davies (1964) in which the screw component of superlattice dislocation tends to cross-slip onto another {111} plane to decrease the energy of antiphase boundary (APB)on a {100} plane. Because any further movement of either component produces APB the dislocation becomes sessile and forms an obstacle for other glissile dislocations. For temperatures below the peak in $\frac{d\sigma}{d\varepsilon}$, rate of formation of such obstacles increases with temperature (since cross-slip of one of the unit dislocations of the superdislocation is thermally activated). At higher temperatures both the dislocations composing the superdislocation can cross-slip onto {111} with the result of no barriers formed. Stoloff and Davies (1966) present micrographic evidence to support their conclusions.

6. CONCLUSIONS

At the temperatures where serrations were observed in the present case of Cu_3Au, annealing of vacancies has only a minute effect on the total

vacancy concentration. Equilibrium vacancy concentration at these temperatures is also negligible compared to that due to straining. Thus an application of modified Cottrell equation yielded activation energies for serrated flow equal to those for vacancy migration in ordered and disordered alloys. The activation energies for dynamic strain-ageing in both these states at the disappearance of serrations are found to be equal to the sum of the activation energy for self-diffusion and the binding energy of solute atoms to dislocations. Deduced values for $(m + \beta)$ in both disordered and ordered states are comparable to those obtained on other alloy systems.

The many areas of agreement between experimental results and theoretical predictions notwithstanding, the yield stress and strain-hardening coefficient and their temperature dependencies cannot be accounted for by, for example, Cottrell-Jaswon model. The complicated temperature dependencies of yield stress and $\frac{d\sigma}{d\varepsilon}$ are thought to have arisen from simultaneous occurrence of short or long-range ordering as well as strain-ageing. Predictions based on Mott-Nabarro and Li's models of solid-solution hardening combined with change in the degree of order (for ordered) or with short-range ordering reaction (in originally disordered) explain, at least qualitatively, the observed temperature dependence of the yield stress.

References

Ardley, G. H., 1955, Acta Metall., 3, 525.

Benci, S., Gasparini, G., and Germagnoli, E., 1964, Nuovo Cemento, 31, 1165.

Blewitt, T. H., Cottman, R. R., and Redman, J. K., 1955, Phys. Soc. (Lond.), 359.

Bird, J. E., Mukherjee, A. K., and Dorn, J. E., 1969, "Quantitative Relation between Properties and Microstructure," Proceedings of an International Conference, Haifa, Israel, p. 255.

Brindley, B. J., and Worthington, P. J., 1969, Acta Metall., 17, 1357.

Van Bueren, H. G., 1955, Acta Metall. 3, 519.

Charnock, W., 1969, Phil. Mag., 18, 89.

Cottrell, A. H., 1948, "Report on the Strength of Solids," The Physical Society, London, p. 30; 1953 a, "Relation of Properties to Microstructure," ASM Symposium, p. 14; 1953b, Phil. Mag. 15, 829.

Cottrell, A. H., and Bilby, B. A., 1949, Proc. Phy. Soc., 219, 328.

Cottrell, A. H., and Jaswon, M. A., 1949, Proc. R. Soc. A., 199, 104.

Fisher, J. C., 1954, Acta Metall. 2, 9.

Ham, R. K., and Jaffrey, D., 1967, Phil. Mag. 15, 247.

Johnston, W. G., and Gilman, J. J., 1959, J. Appl. Phys., 30, 129.

Keh, A. S., Nakada, Y., and Leslie, W. C., 1968, "Dislocation Dynamics," (New York: Mc Graw-Hill), p. 381.

Langdon, T. G., and Dorn, J. E., 1968, Phil. Mag., 17, 999.

Li, J. C. M., 1968, "Dislocation Dynamics," (New York: McGraw-Hill) p. 87.

MacEwen, S. R., and Ramaswami, B., 1970, Phil. Mag., 22, 1025.

McCormick, P. G., 1971, Phil. Mag., 24, 949.

Mohamed, F. A., (1970), (M.S. Thesis), UCRL Report 1921, Lawrence Berkeley Laboratory, University of California, Berkeley.

Mott, N. F., 1952, Phil. Mag. 43, 1151.

Mukherjee, K., D'Antonio, C., Maciag, R., and Fisher, G., 1968, J. Appl. Phys, 39, 5434.

Murty, K. Linga, and Dorn, J. E., 1971, "Effect of Vacancy Sinks and Sources on Serrated Yielding due to Solute Locking," to be published in Scripta Met.

Nakada, Y., and Keh, A. S., 1970, Acta Metall., 18, 437.

Rider, J. G., and Faxon, C. J. B., 1966, Phil. Mag., 13, 289.

Russell, B., 1963, Phil. Mag., 8, 615.

Schoeck, G., and Seeger, A., 1959, Acta Metall., 7, 469.

Seitz, F., 1952, Advanc. Phys., 1, 43.

Soler-Gomez, A. J. R., and Mc G. Tegart, W. J., 1969, Phil. Mag., 20, 495.

Stoloff, N. S., and Davies, R. G., 1964, Phil. Mag., 9, 349; 1965, Trans. AIME, 233, 1500; 1966, Prog. Mater. Sci., 13, 3.

Suzuki, H., 1952, Science Reports, Research Institute, Tohoku University, A, 4, 455.

Wazzan, A. R., and Dorn, J. E., 1965, J. Appl. Phys., 36, 222.

Table 1

Serrations in various temperature regions:

Range Of Temperature °K		Is σ-ε curve serrated?	Comments
DISORDERED	ORDERED		
<308	≤ 355	no	completely smooth
310 - 410	360 - 426	yes	only after a finite strain
414 - 513	450 - 520	yes	completely serrated
515 - 570	523 - 530	yes	slightly serrated and only type C observed
≥ 575	533 - 653	no	completely smooth

Table 2

- Experimental Values of $(m + \beta)$ in Various Alloys -

Alloy	$m + \beta$	Reference
Cu - Sn	2.2	Ham and Jaffrey (1967); Russell (1963)
Au - In	2.14 - 3	Soler-Gomez and Mc G. Tegart (1969)
Brass	1.9	Charnock (1969)
Al - Mg	1.7	MacEwen and Ramaswami (1970)
7075 Al	3.0	Mukherjee et al (1968)
Cu_3Au		
Disordered	2.18	Present study
Ordered	2.98	Present study
Theory	2 - 3	Van Bueren (1955), Ham and Jaffrey (1967)

Table 3

- Activation Energies for Diffusion in Ordered and Disordered Alloys -

	Structure	E_D kCal/mole	Ratio E_D^{ORD}/E_D^{DIS}	Reference
β - Brass	Ord. bcc Dis. bcc	38.3 23.4	1.63	Hren[1]
Fe-Al-Si	Ord. Dis.	90.0 77.0	1.17	Schmatz and Zackay[2]
Mg Cd	Ord. hcp. Dis. orth.	33.5 28.6	1.17	Soler-Gomez and Tegart[3]
Fe_3Al	Ord. bcc Dis. bcc	92.0 78.0	1.18	Lawley, Coll and Cahn[4]
Cu_3Au	Ord. sc Dis. fcc	49.8 39.7	1.26	Present study
Cu_3Au	Ord. sc Dis. fcc	22.1* 17.9*	1.23	Present Study

* Value for Em

1. J. A. Hren, Ph. D. Thesis, Stanford University (1962).

2. D. J. Schmatz and V. F. Zackay, Trans. ASM, 51 299 (1959).

3. Soler-Gomez and Mc G. Tegart (1964).

4. A. Lawley, J. A. Coll and R. W. Cahn, Trans. AIME, 218, 166 (1960).

Figure Captions

1. Load vs elogation curves for disordered state. The three types of serrations (A, B and C) are depicted in the inset.
2. Load vs elogation curves for ordered state.
3. Plot of $\Delta\sigma$ as a function of strain.
4. Dependence of $\Delta\varepsilon$ on strain.
5. Plot of $\Delta\sigma$ vs ageing time.
6. Double-log plot of strain rate versus delay in strain for the occurrence of serrations in both ordered and disordered alloys.
7. Arrhenius plot of the delay in strain (ε_o) for ordered and disordered states.
8. Plot of ln $\dot{\varepsilon}$ vs 1/T for the disappearance of serrations.
9. Temperature dependence of yield stress.
10. Temperature dependence of strain-hardening coefficient $(\frac{d\sigma}{d\varepsilon})$.
11. Plot of ln $\Delta\sigma_t$ vs $\ln\left\{\frac{\exp(-E_m/RT)}{T}\right\}$ to prove the validity of Cottrell-Bilby equation for the strain ageing kinetics of type A in disordered state.
12. Plot of ln $\dot{\varepsilon}$ vs $\frac{1}{T}$.
13. Temperature dependence of the degree of order in Cu_3Au.

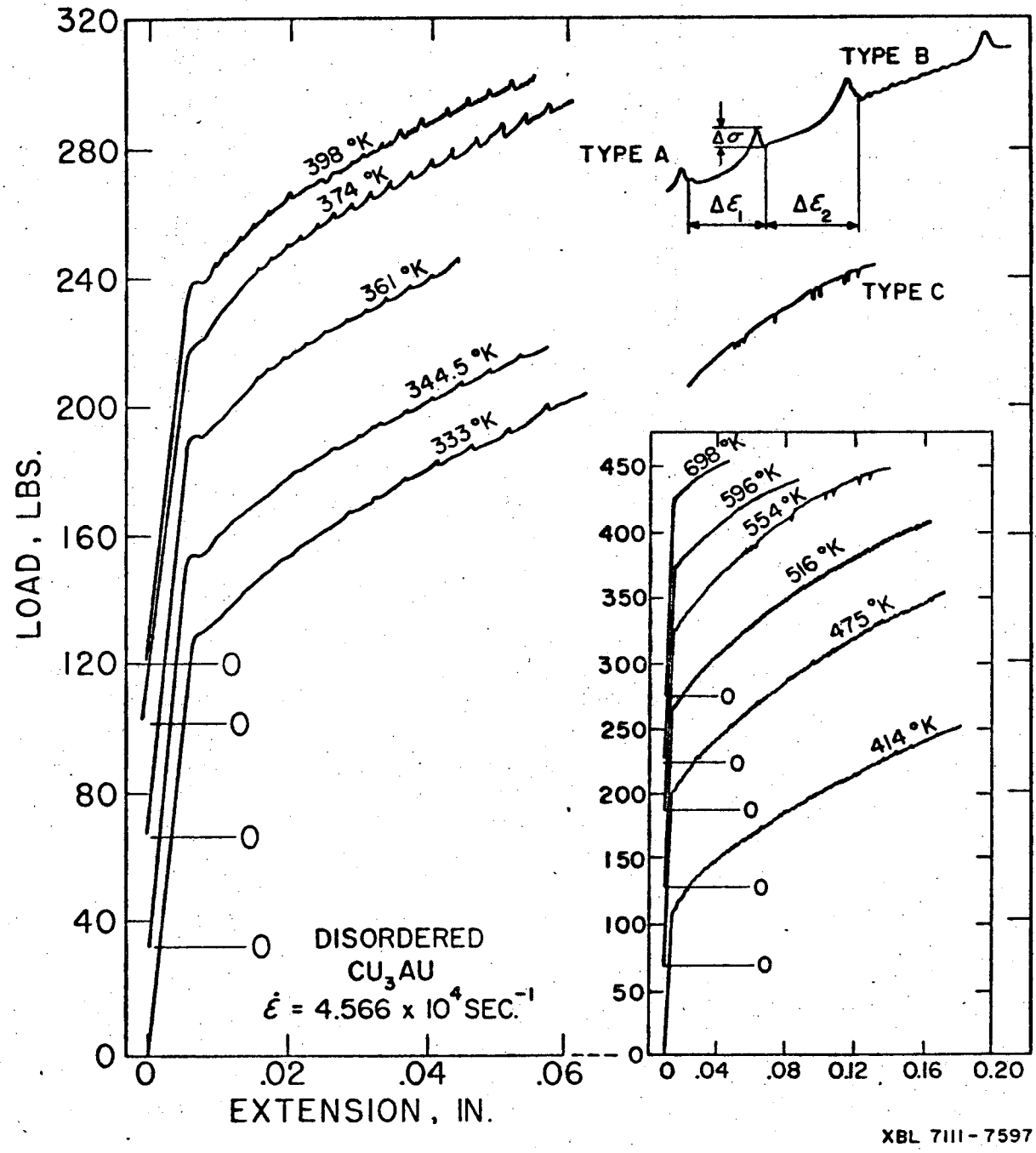
LOAD, LBS.
EXTENSION, IN.
398 °K
374 °K
361 °K
344.5 °K
333 °K
DISORDERED
CU3AU
ε̇ = 4.566 x 10⁴ SEC.⁻¹
TYPE A
TYPE B
TYPE C
Δσ
Δε1
Δε2
698 °K
596 °K
554 °K
516 °K
475 °K
414 °K
XBL 7111-7597

Fig. 1

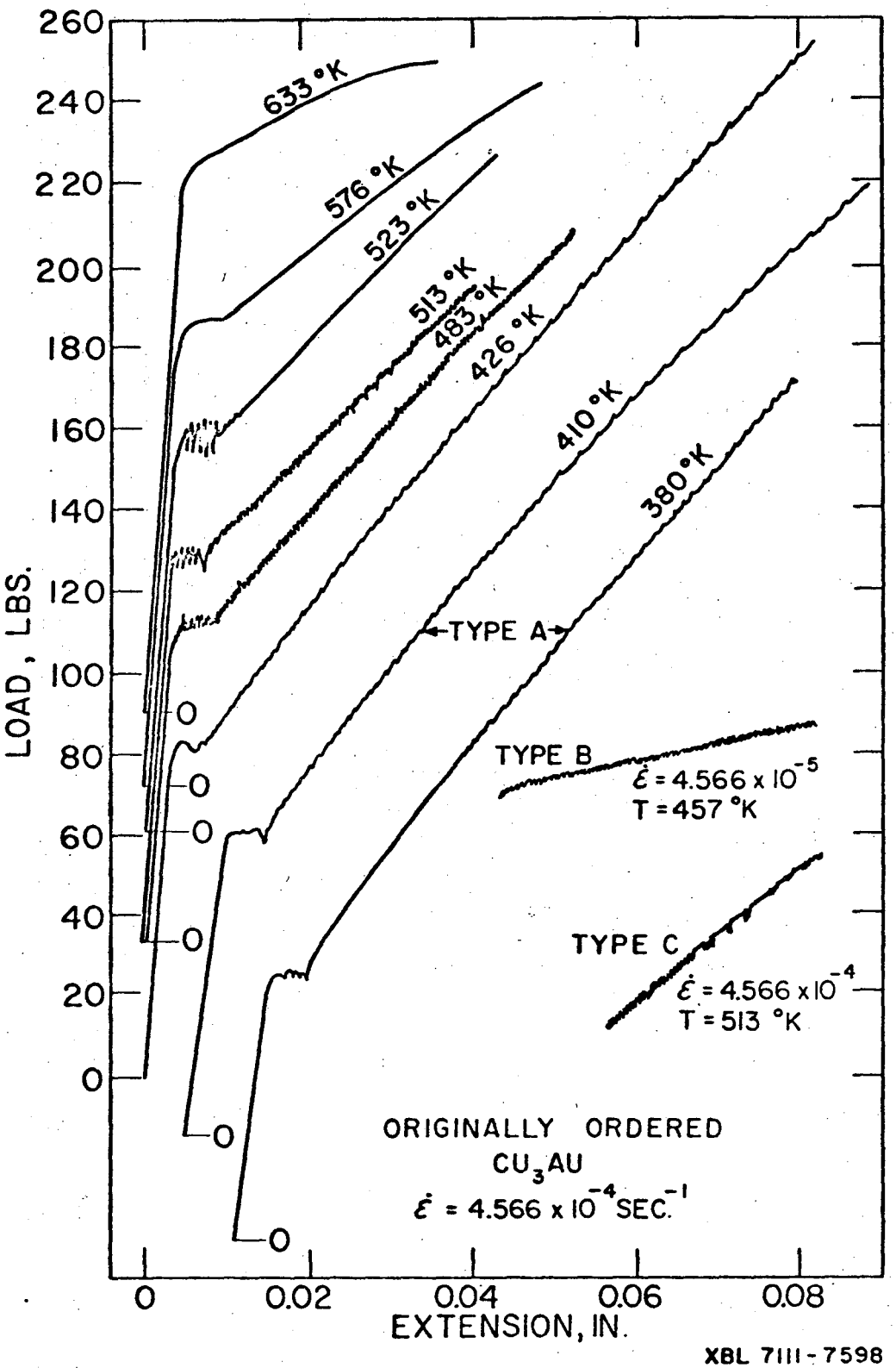
LOAD, LBS.
260
240
220
200
180
160
140
120
100
80
60
40
20
0
633°K
576°K
523°K
513°K
483°K
426°K
410°K
380°K
TYPE A
TYPE B
$\dot{\varepsilon} = 4.566 \times 10^{-5}$
T = 457 °K
TYPE C
$\dot{\varepsilon} = 4.566 \times 10^{-4}$
T = 513 °K
ORIGINALLY ORDERED
CU_3AU
$\dot{\varepsilon} = 4.566 \times 10^{-4} SEC.^{-1}$
0
0.02
0.04
0.06
0.08
EXTENSION, IN.
XBL 7111-7598

Fig. 2

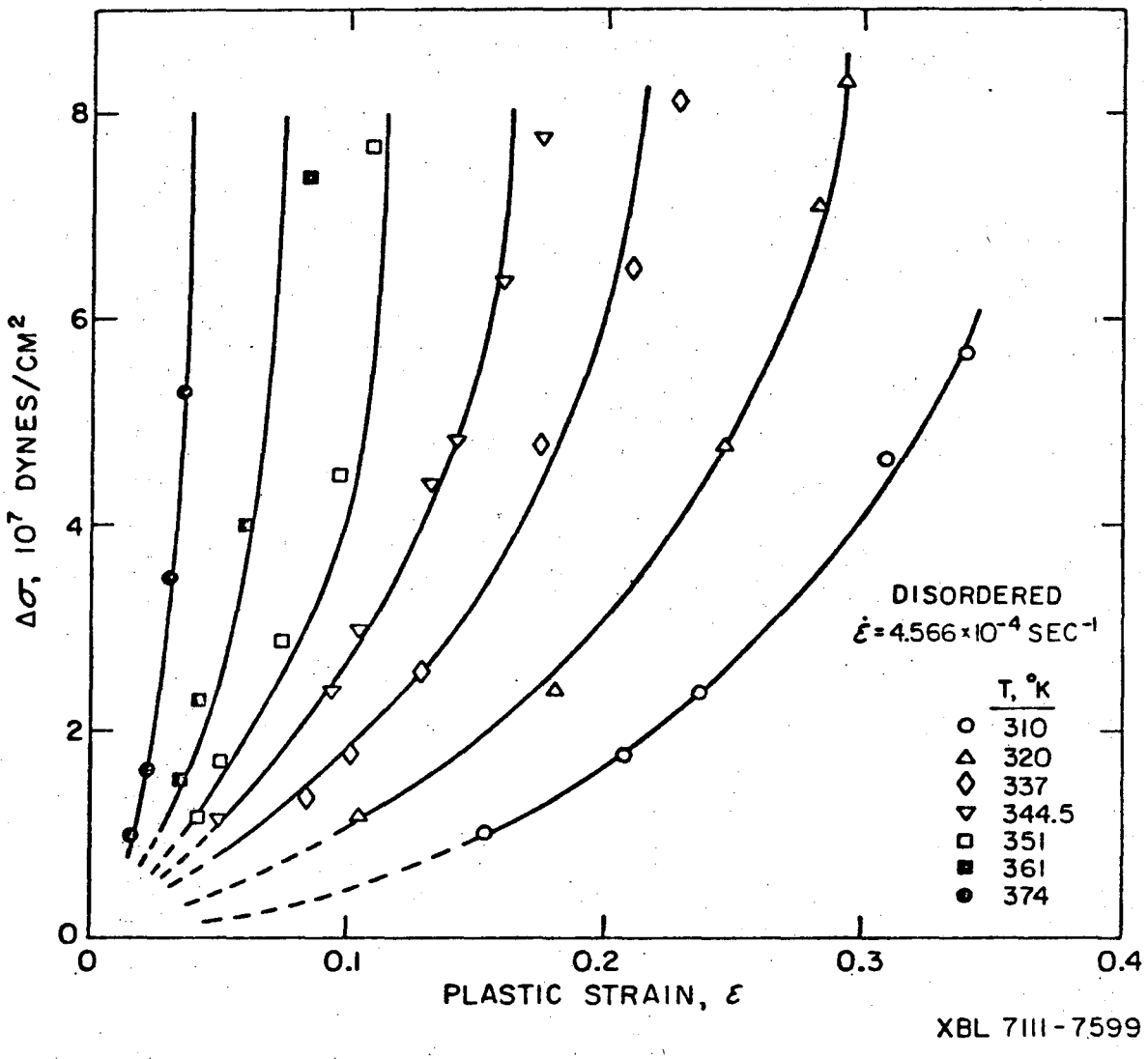
Δσ, 10⁷ DYNES/CM²
PLASTIC STRAIN, ε
0
2
4
6
8
0
0.1
0.2
0.3
0.4
DISORDERED
ε̇ = 4.566 × 10⁻⁴ SEC⁻¹
T, °K
310
320
337
344.5
351
361
374
XBL 7111-7599

Fig. 3

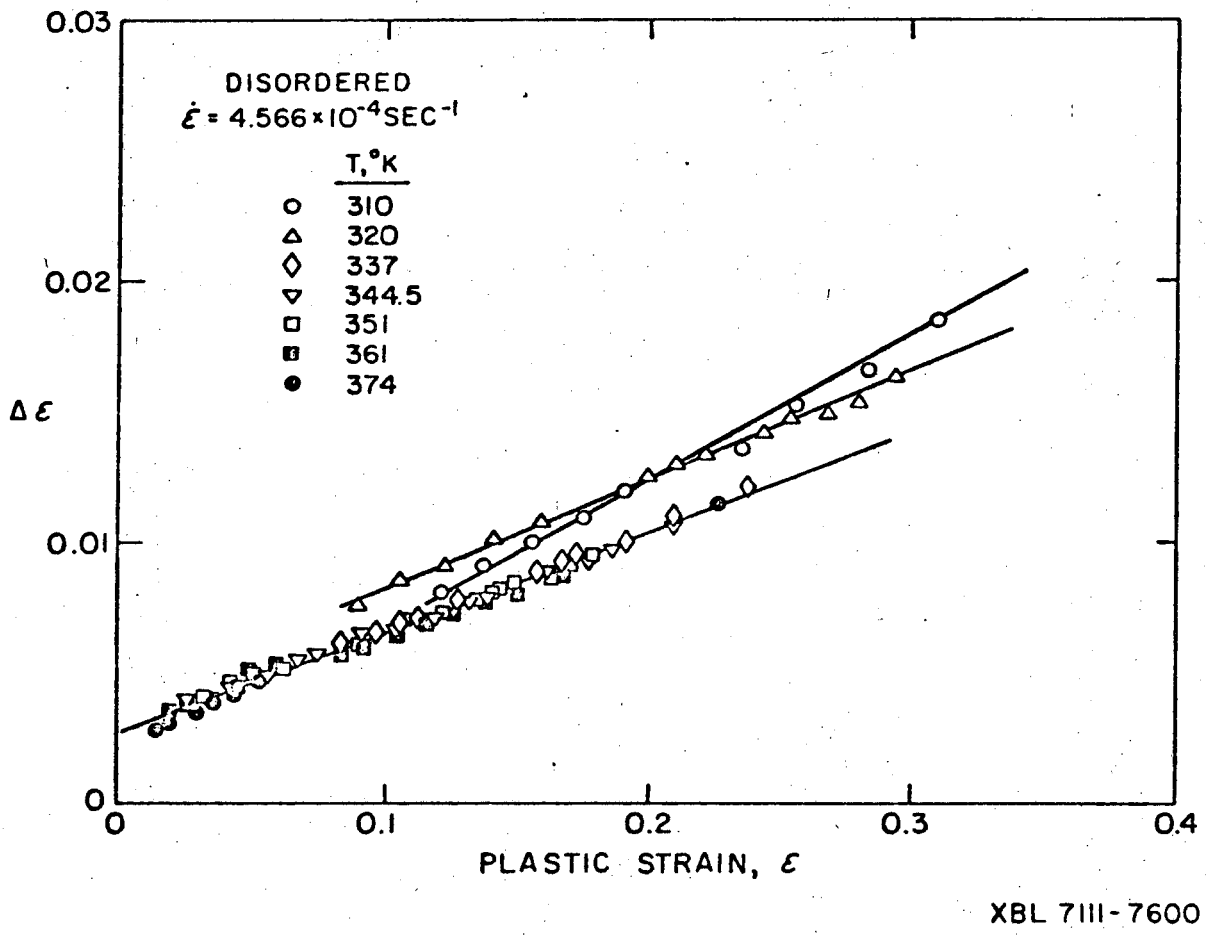
DISORDERED
$\dot{\varepsilon} = 4.566 \times 10^{-4} SEC^{-1}$
T, °K
310
320
337
344.5
351
361
374
0.03
0.02
0.01
0
$\Delta\varepsilon$
0
0.1
0.2
0.3
0.4
PLASTIC STRAIN, ε
XBL 7111-7600

Fig. 4

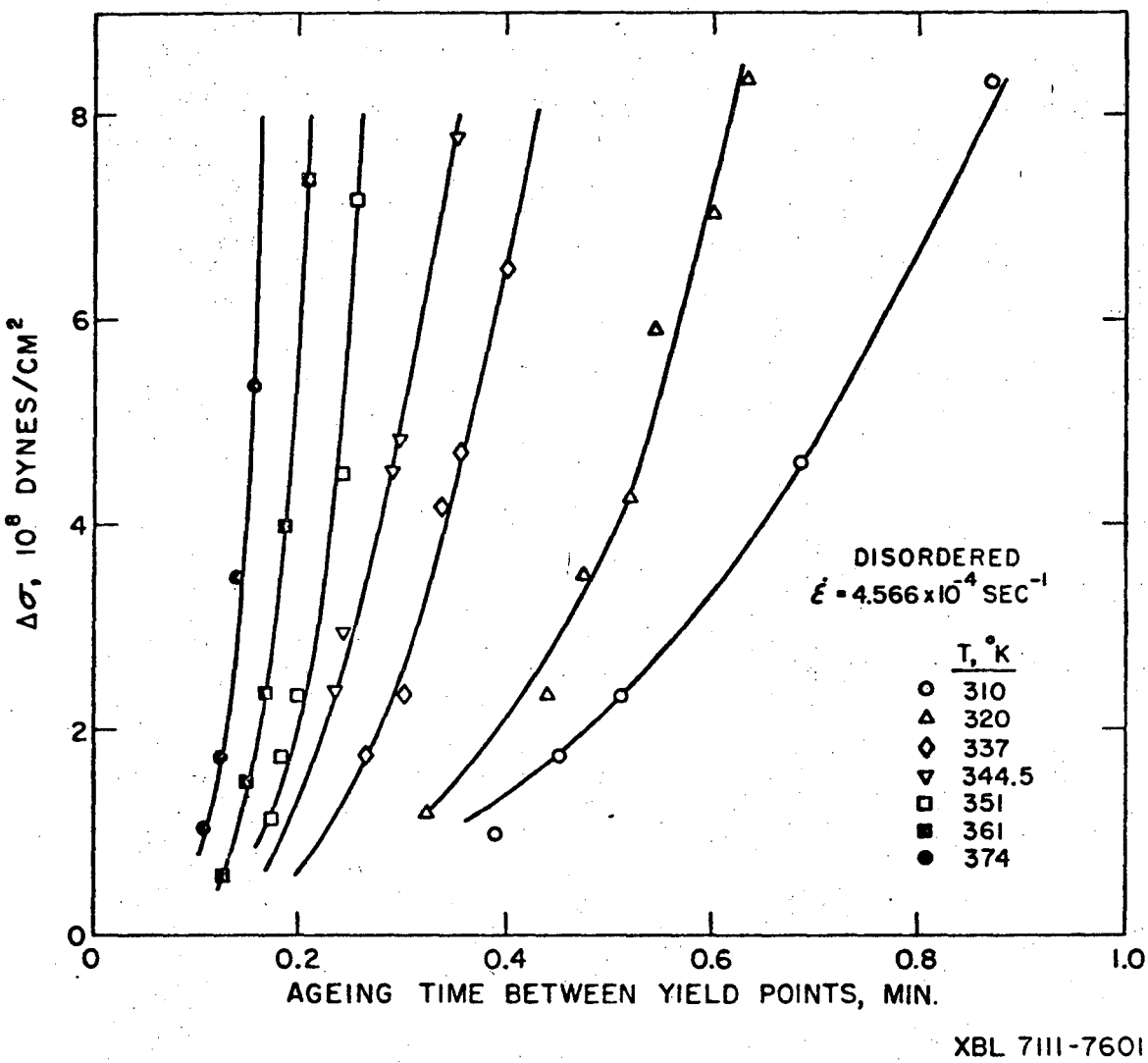
Δσ, 10⁸ DYNES/CM²
AGEING TIME BETWEEN YIELD POINTS, MIN.
DISORDERED
ε̇ = 4.566×10⁻⁴ SEC⁻¹
T, °K
310
320
337
344.5
351
361
374
XBL 7111-7601

Fig. 5

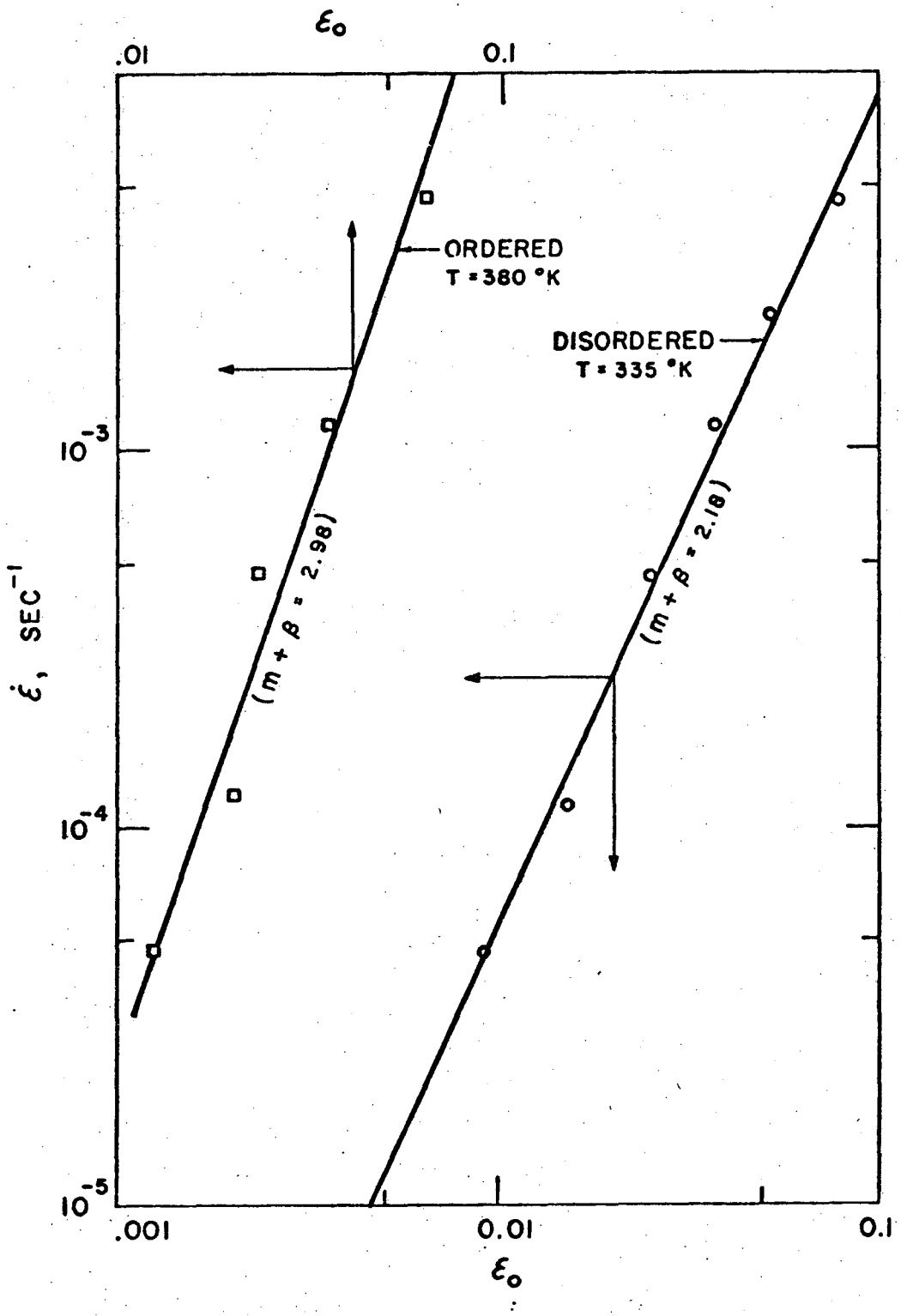

XBL 7111-7602

Fig. 6

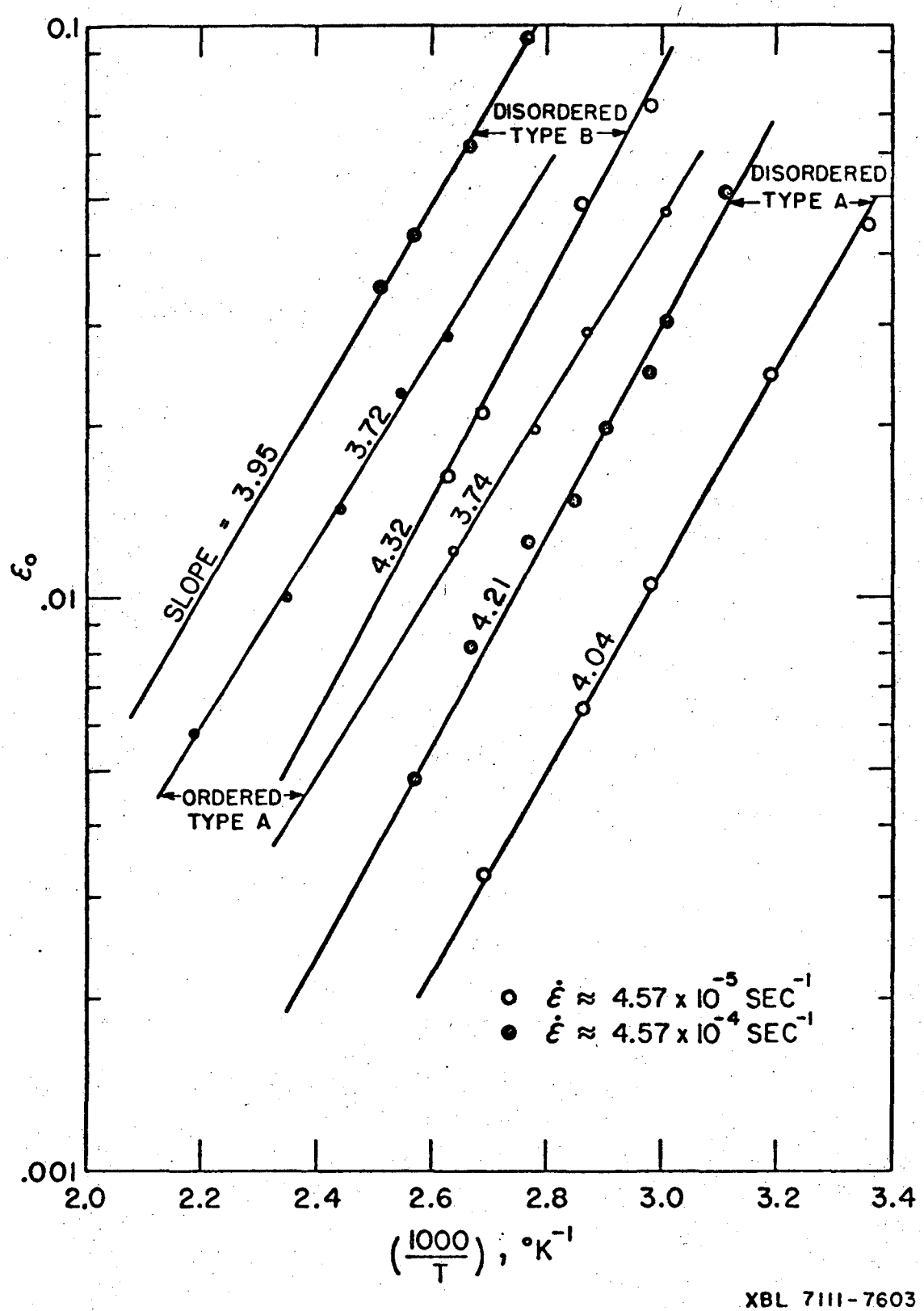
0.1
.01
.001
$\dot{\varepsilon}_o$
DISORDERED
TYPE B
DISORDERED
TYPE A
ORDERED
TYPE A
SLOPE = 3.95
3.72
4.32
3.74
4.21
4.04
$\dot{\varepsilon} \approx 4.57 \times 10^{-5}$ SEC^{-1}
$\dot{\varepsilon} \approx 4.57 \times 10^{-4}$ SEC^{-1}
2.0
2.2
2.4
2.6
2.8
3.0
3.2
3.4
$\left(\frac{1000}{T}\right)$, °K^{-1}
XBL 7111-7603

Fig. 7

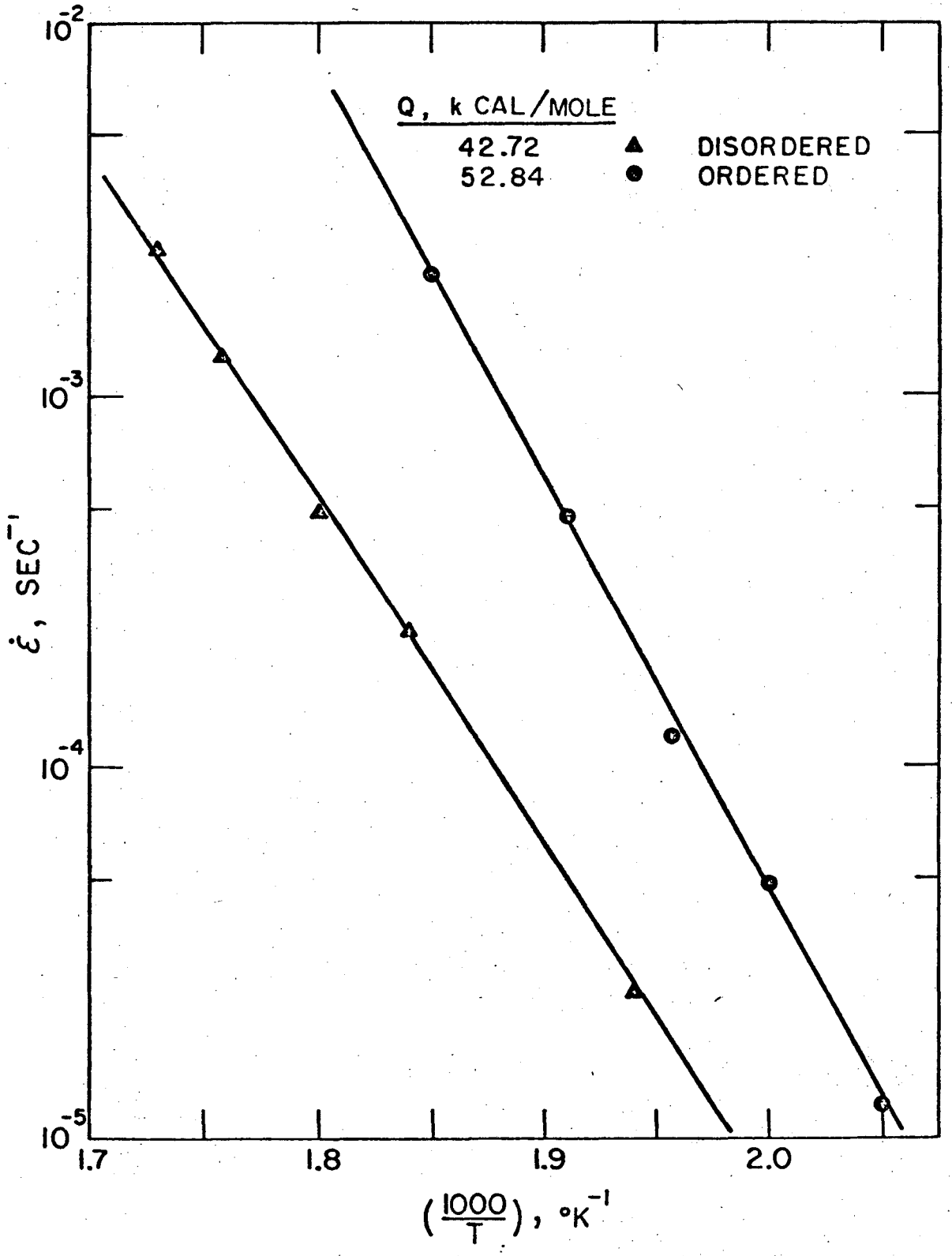

XBL 7111-7604

Fig. 8

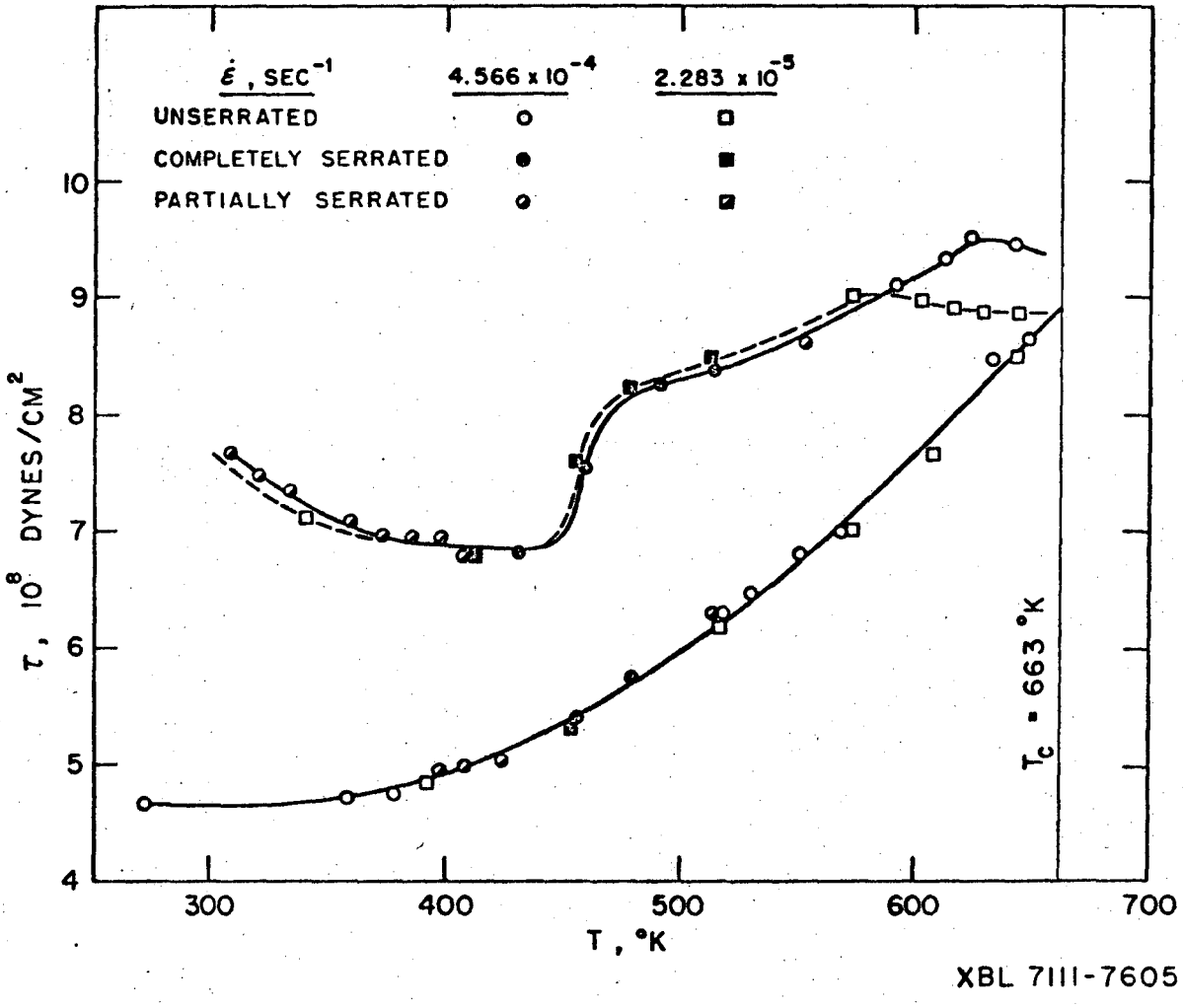
$\dot{\epsilon}$, SEC^{-1}
4.566 x 10^{-4}
2.283 x 10^{-5}
UNSERRATED
COMPLETELY SERRATED
PARTIALLY SERRATED
τ, 10^8 DYNES/CM^2
T, °K
T_c = 663 °K
XBL 7111-7605

Fig. 9

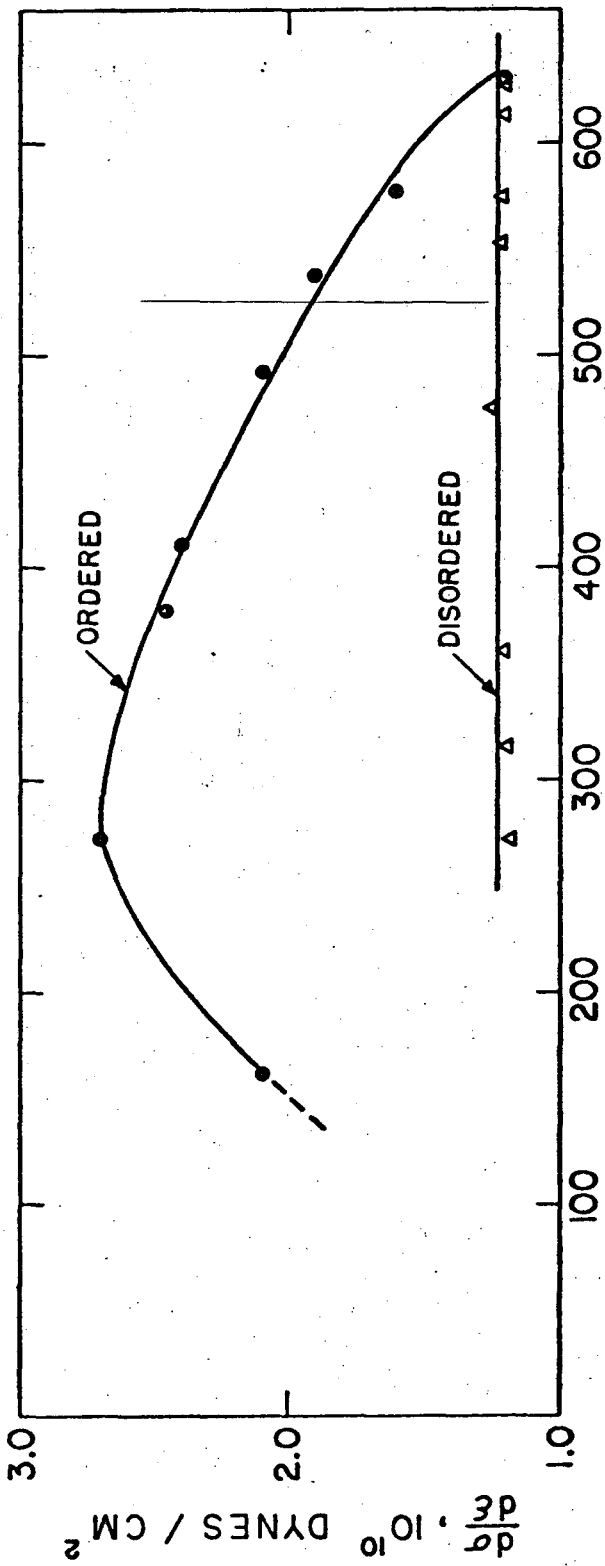

XBL 7111-7606

Fig. 10

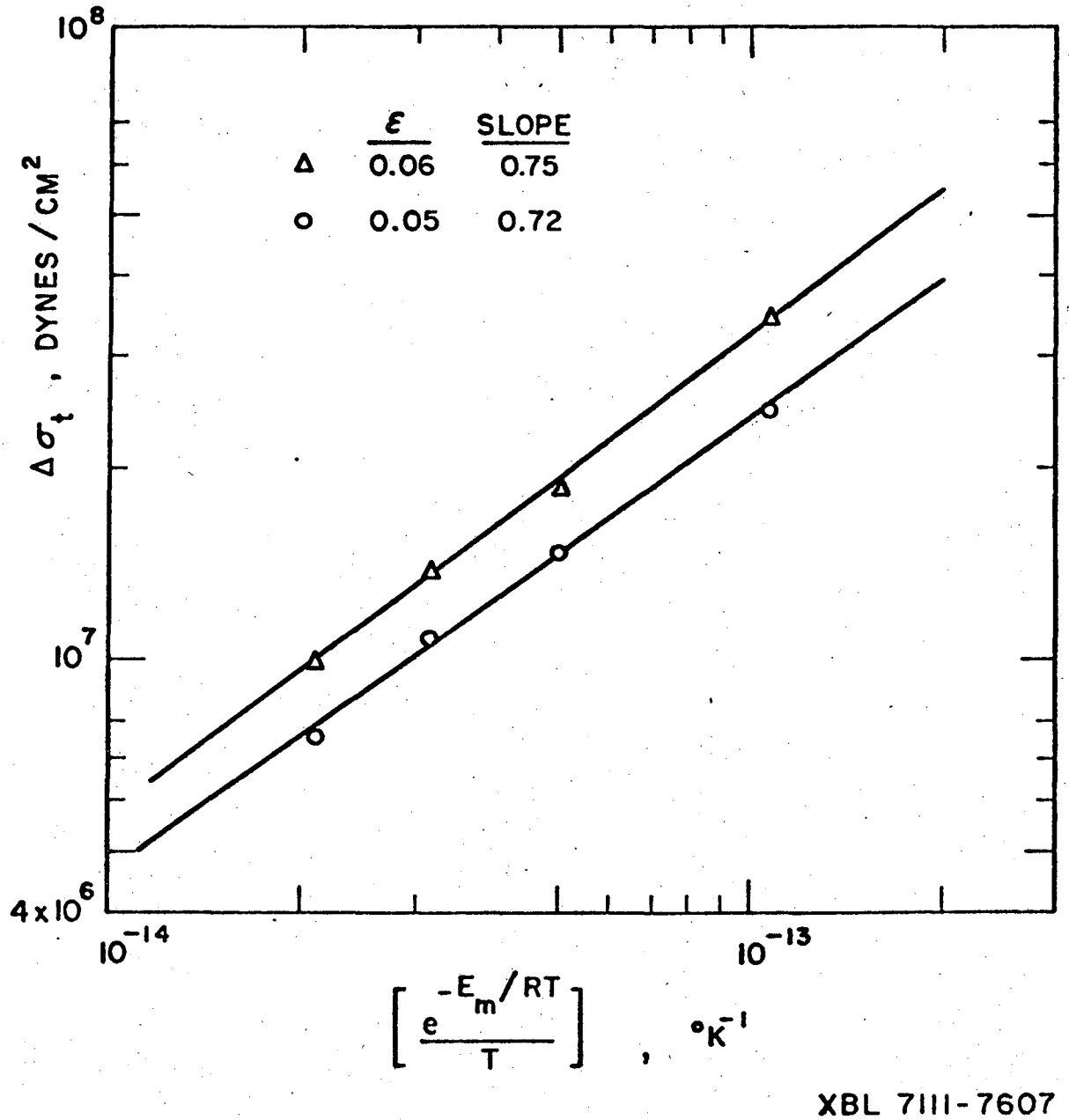
10^8
10^7
4×10^6
$\Delta\sigma_t$, DYNES / CM^2
ε SLOPE
Δ 0.06 0.75
o 0.05 0.72
10^{-14}
10^{-13}
$\left[\frac{e^{-E_m/RT}}{T}\right]$, °K^{-1}
XBL 7111-7607

Fig. 11

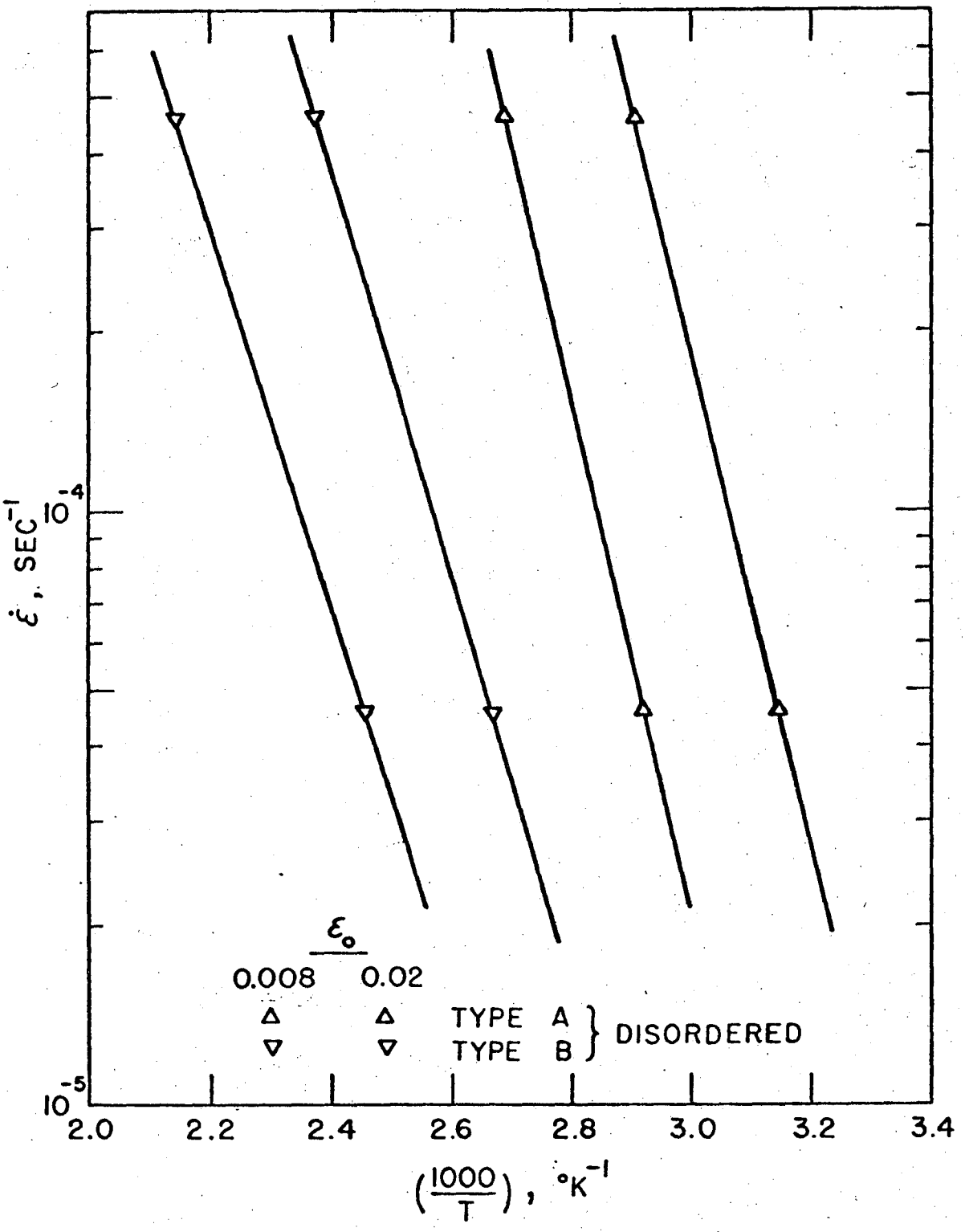
$\dot{\varepsilon}$, SEC^{-1}
10^{-4}
10^{-5}
ε_o
0.008
0.02
TYPE A
TYPE B
DISORDERED
2.0
2.2
2.4
2.6
2.8
3.0
3.2
3.4
$\left(\frac{1000}{T}\right)$, °K^{-1}
XBL 7111-7609

Fig. 12

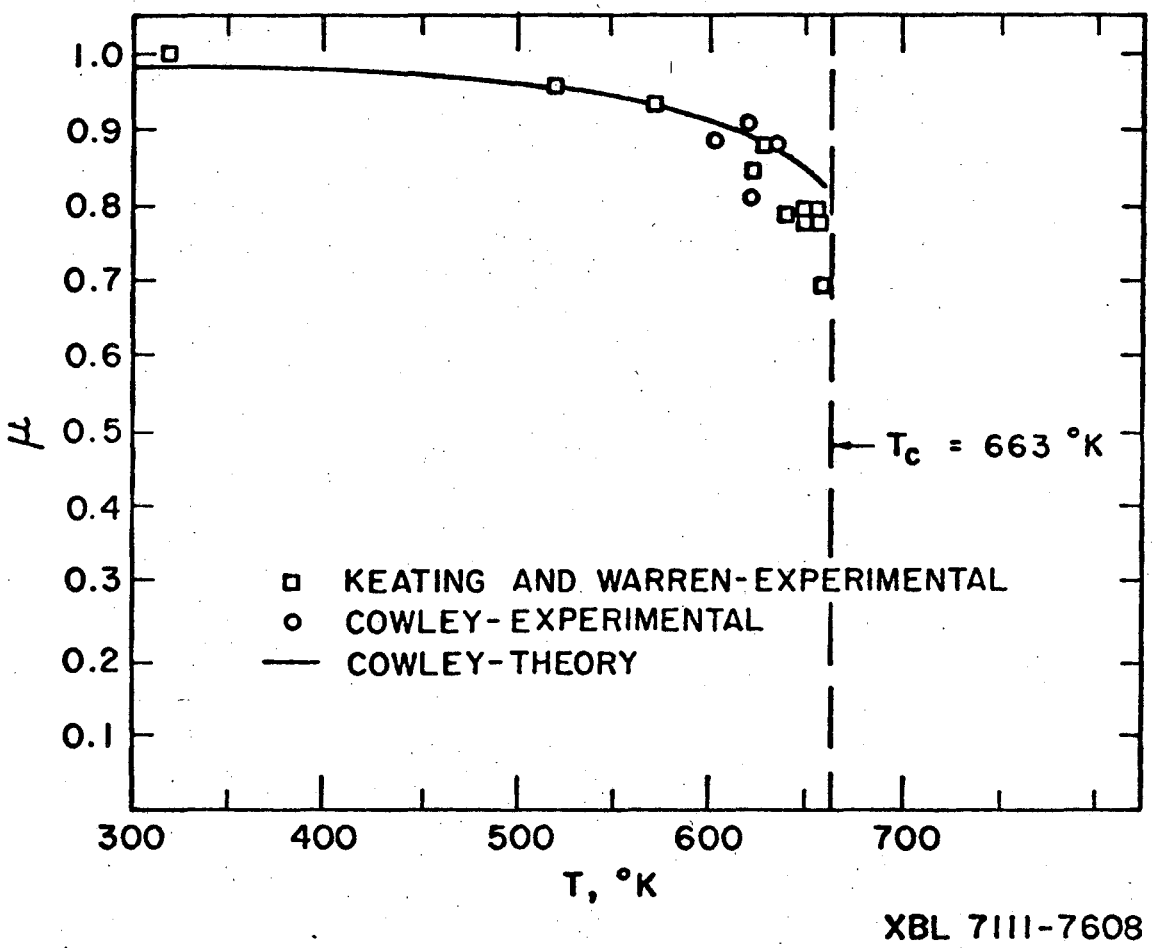
1.0
0.9
0.8
0.7
0.6
0.5
0.4
0.3
0.2
0.1
μ
T_c = 663 °K
KEATING AND WARREN-EXPERIMENTAL
COWLEY-EXPERIMENTAL
COWLEY-THEORY
300
400
500
600
700
T, °K
XBL 7111-7608

Fig. 13

TECHNICAL INFORMATION DIVISION
LAWRENCE BERKELEY LABORATORY
UNIVERSITY OF CALIFORNIA
BERKELEY, CALIFORNIA 94720